

# Boost DC–AC Inverter: A New Control Strategy

Pablo Sanchis, *Member, IEEE*, Alfredo Ursæa, *Member, IEEE*, Eugenio Gubía, *Member, IEEE*, and Luis Marroyo, *Member, IEEE*

**Abstract**—Boost dc–ac inverter naturally generates in a single stage an ac voltage whose peak value can be lower or greater than the dc input voltage. The main drawback of this structure deals with its control. Boost inverter consists of Boost dc–dc converters that have to be controlled in a variable-operation point condition. The sliding mode control has been proposed as an option. However, it does not directly control the inductance averaged-current. This paper proposes a control strategy for the Boost inverter in which each Boost is controlled by means of a double-loop regulation scheme that consists of a new inductor current control inner loop and an also new output voltage control outer loop. These loops include compensations in order to cope with the Boost variable operation point condition and to achieve a high robustness to both input voltage and output current disturbances. As shown by simulation and prototype experimental results, the proposed control strategy achieves a very high reliable performance, even in difficult transient situations such as nonlinear loads, abrupt load changes, short circuits, etc., which sliding mode control cannot cope with.

**Index Terms**—Control systems, dc–ac power conversion, inverters, power conversion, power electronics, power generation, power system control.

## I. INTRODUCTION

THE Boost dc–ac inverter, also known as Boost inverter, consists of two individual Boost converters, as shown in Fig. 1. In this topology, both individual Boosts are driven by two 180° phase-shifted dc-biased sinusoidal references whose differential output is an ac output voltage [1], [2]. As a consequence, the peak value of this ac voltage can be lower or greater than the dc input voltage. The idea of controlling the phase-shift between two Boost dc–dc converters in order to achieve a dc–ac inverter is also provided by the theory of phase-modulated inverters, which is presented and analyzed in [3]. The Boost dc–ac inverter exhibits several advantages, the most important of which is that it can naturally generate an ac output voltage from a lower dc input voltage in a single power stage. The reduced number of switches that is required (only four) and the quality of the output voltage sine wave are additional advantages that have been often mentioned in the literature [1], [2], [4], [5].

The control of the ac output voltage requires controlling both Boost converters. However, the Boost converter is a difficult system to be controlled. Several methods based on the small-signal linear model have been designed to control the Boost

around a particular operation point, for which the model is calculated [6]–[8]. However, these methods are not appropriate to control the individual Boosts of the inverter because now the operation point experiments large variations and so do the small-signal model parameters.

The sliding mode control has been proposed to control the Boost inverter. This control strategy can deal with variable operation point conditions and can therefore be applied to both individual Boost converters [2], [4]. The sliding mode control achieves good steady state results. However, it has some disadvantages related to the required complex theory, the variable switching frequency, the lack of an inductance averaged-current control and the constraints to the controller parameter selection [5].

This paper proposes a control strategy for the Boost inverter in which each Boost is controlled by means of a double-loop control scheme that consists of a new inductor current control inner loop and an also new output voltage control outer loop [9], [10]. Both control loops are based on the averaged continuous-time model of the Boost topology [11]. The proposed control loops include several compensations in order to decouple the converter model seen by the controller from the operation point. In so doing, the control is able to deal with the variable operation condition of both Boosts. In order to improve the system robustness against external disturbances, feedforward control techniques have been proposed and applied to the Boost dc–dc converter [12]–[14]. With the same aim, additional feed-forward regulations are included in the proposed control loops that make the controlled system be robust to both dc input voltage and ac output current disturbances, what represents an additional advantage. As it will be shown through this paper, the direct control of the current makes possible to cope with special situations that cannot be tackled by the sliding mode control, such as nonlinear loads, abrupt load variations, and transient short circuit situations, keeping the inverter in a stable operating condition by means of limiting the inductor current. Because of this ability to keep the system under control even in these situations, the inverter achieves a very reliable operation. On the contrary, the sliding mode control is not able to deal with these situations, as it does not control the inductor current. A prototype has been designed and physically developed. Simulation and experimental results, including those special situations mentioned before, show the good performance of this new control strategy and its better characteristics in comparison with the sliding mode control.

## II. DOUBLE-LOOP CONTROL SCHEME FOR THE BOOST

The averaged model describes the dynamic behavior of the Boost up to frequencies below the switching frequency, typi-

Manuscript received October 8, 2003; revised July 30, 2004. This paper was presented in part at the 32nd IEEE-PESC'01 Conference, Vancouver, Canada, June 17–21, 2001. Recommended by Associate Editor M. Vitelli.

The authors are with the Department of Electrical and Electronic Engineering, Universidad Publica de Navarra, Pamplona 31006, Spain (e-mail: pablo.sanchis@unavarra.es).

Digital Object Identifier 10.1109/TPEL.2004.843000

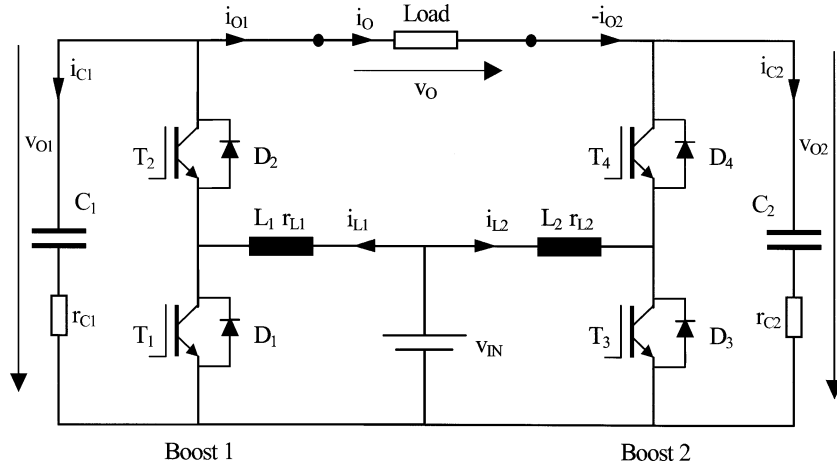


Fig. 1. Boost dc-ac inverter.

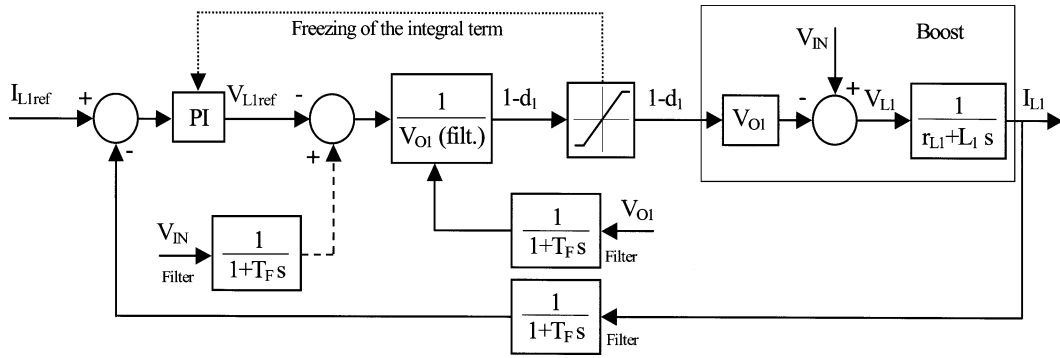


Fig. 2. Proposed inductor current control loop.

cally below half this frequency [11]. The model equations particularized for the Boost 1 are described as follows:

$$v_{IN} - v_{L1} = (1 - d_1)v_{O1} \quad (1)$$

$$i_{C1} + i_{O1} = (1 - d_1)i_{L1} \quad (2)$$

where  $v_{O1}$  and  $i_{C1}$  are the capacitor voltage and current,  $v_{L1}$  and  $i_{L1}$  the inductor voltage and current,  $v_{IN}$  the input voltage,  $i_{O1}$  the output current, and  $d_1$  the duty cycle time-averaged value. Subscript 1 denotes Boost 1.

The inductor and capacitor differential equations are

$$v_{L1} = r_{L1}i_{L1} + L_1 \frac{di_{L1}}{dt} \quad (3)$$

$$i_{C1} + r_{C1}C_1 \frac{di_{C1}}{dt} = C_1 \frac{dv_{O1}}{dt} \quad (4)$$

where  $L$ ,  $C$ ,  $r_L$ , and  $r_C$  are the values for the inductance, capacity, and inductor and capacitor equivalent series resistance, respectively.

From (1) and (2), the duty cycle can be worked out, and then, by means of (3) and (4), the following expression can be obtained, in which internal resistances have been neglected:

$$\left( v_{IN} - L_1 \frac{di_{L1}}{dt} \right) i_{L1} = \left( i_{O1} + C_1 \frac{dv_{O1}}{dt} \right) v_{O1}. \quad (5)$$

The last expression shows the Boost dynamic bilinear behavior and the difficulty of designing an accurate and robust controller for this converter suitable for any operation point, as

it is required in the Boost inverter. In order to deal with these problems, and as an alternative to the sliding mode control, a double-loop control strategy is proposed that consists of a new inductor current control inner loop and an also new capacitor voltage control outer loop. Both loops are shown in Figs. 2 and 3 particularized for Boost 1.

The plant to be controlled in the inductor current control loop shown in Fig. 2 is defined by (1) and (3). In variable operation conditions, these equations show a nonlinear system that depends on the output voltage ( $v_{O1}$ ), and in which the input voltage ( $v_{IN}$ ) appears as an external disturbance. If the duty cycle were the controller output, i.e., the control variable, the plant seen by the controller would exhibit a variable gain caused by the variable output voltage. Therefore, the control variable is chosen to be the inductor voltage ( $v_{L1}$ ), and then the plant seen by the converter is simply the Laplace transformation of (3). With this strategy, the input voltage influence is also cancelled. The duty cycle ( $d_1$ ) is then obtained by means of the following expression, in which  $v_{L1ref}$  is the controller output

$$1 - d_1 = \frac{v_{IN} - v_{L1ref}}{v_{O1}}. \quad (6)$$

From a different point of view, the proposed control strategy compensates the variable gain of the plant (the output voltage  $v_{O1}$ ) by means of a gain that is the inverse value of this output voltage, and cancels the influence of the input voltage ( $v_{IN}$ ) by adding again to the control loop this disturbance with its opposite value. The compensation of the output voltage can be done

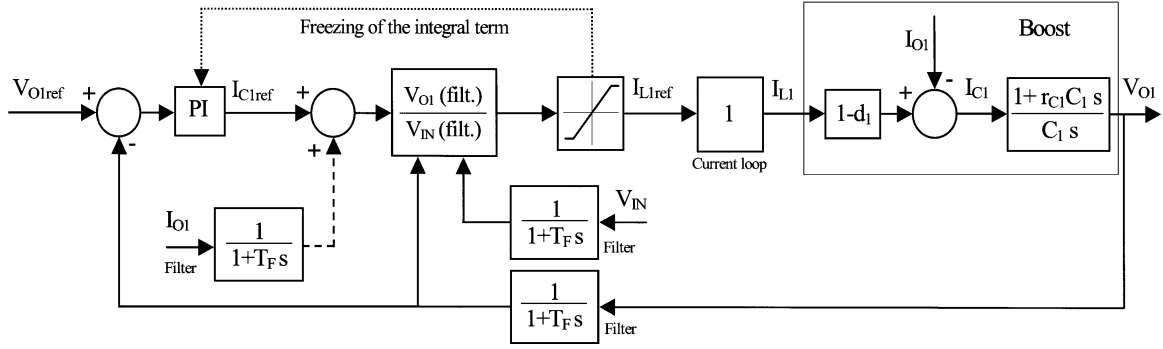


Fig. 3. Proposed output voltage control loop.

due to the much higher current loop bandwidth in comparison with the output voltage bandwidth. The cancellation of the input voltage influence acts in fact as a feed-forward control. This cancellation would not be required if the current loop bandwidth is much faster than the input voltage dynamics. The controller is a proportional-integral controller (PI) that can be easily designed by traditional methods. Variables are filtered and the duty cycle is limited in order to avoid too high voltages and noise influences. A freezing action of the controller integral term is activated in case of saturation.

Concerning the output voltage loop, which is introduced in Fig. 3, the plant to be controlled is now defined by (2) and (4). These equations show again a nonlinear behavior that depends on the duty cycle ( $d_1$ ) and the output current ( $i_{O1}$ ). The design of the control structure for the output voltage is based on the same philosophy as the current loop. If the control variable were now the current reference for the inner loop, the plant seen by the controller would show again a variable gain caused by the term  $1 - d_1$ . Therefore, the capacitor current ( $i_{C1}$ ) is now proposed to be the control variable and the plant seen by the controller is just the Laplace transformation of (4). The calculation of the current reference from the capacitor current requires the use of the duty cycle ( $d_1$ ), which appears inside the term  $1 - d_1$  as shown in (2). However, the duty cycle dynamics is provided by the inner current loop, and its use in the current reference calculation would cause a coupling between both inner and outer control loops that could make the system unstable. Although the use of a strongly filtered value of the term  $1/(1 - d_1)$  has been proved with good results, this term can be approximated by  $v_{O1}/v_{IN}$  if the inductor energy variations are neglected. This approximation, that can be done due to the relatively small size of the inductance in power Boost converters, achieves more accurate and fast results. With this compensation strategy, duty cycle variations up to the voltage loop bandwidth will be successfully compensated, and therefore the system will accurately track different voltage references up to the loop bandwidth. The current reference is then given by the following expression, in which the controller output is now the capacitor current reference,  $i_{C1ref}$

$$i_{L1ref} = \frac{i_{C1ref} + i_{O1}}{1 - d_1} \approx \frac{v_{O1}}{v_{IN}} (i_{C1ref} + i_{O1}). \quad (7)$$

The proposed output voltage control loop can also be seen as the result of compensating the plant variable gain (defined by  $1 - d_1$ ) with  $v_{O1}/v_{IN}$ . In addition, the external disturbance

given by the output current  $i_{O1}$  that exhibits the plant is cancelled with the proposed strategy. This cancellation will have a helpful influence on the system performance during quick or sudden load variations. As the inductor current can be considered instantaneously controlled, the final plant to be controlled consists only of the capacitor transfer function provided by (4), and therefore, the proportional-integral controller (PI) can now be designed by simple traditional techniques. Filtering of variables and freezing of the controller integral term are again used with no consequences for the control loop performance.

### III. CONTROL STRATEGY FOR THE BOOST INVERTER

The control of the Boost dc-ac inverter is achieved by implementing the previously described control strategy on both Boosts and driving their output voltages with proper dc-biased sinusoidal references. Three options to generate these references are analyzed below.

Traditionally, both Boosts are driven by the following independent references, obtained from the Boost inverter output voltage reference:

$$v_{Oref} = \sqrt{2}V \sin(2\pi ft) \quad (8)$$

$$v_{O1ref} = V_{DC} + \frac{v_{Oref}}{2} = V_{DC} + \frac{V}{\sqrt{2}} \sin(2\pi ft) \quad (9)$$

$$v_{O2ref} = V_{DC} - \frac{v_{Oref}}{2} = V_{DC} - \frac{V}{\sqrt{2}} \sin(2\pi ft) \quad (10)$$

where  $v_{Oref}$  is the reference for the Boost inverter,  $v_{O1ref}$  and  $v_{O2ref}$  are the references for both individual Boost converters, respectively,  $f$  and  $V$  are the frequency and rms-value of the ac output voltage, respectively, and  $V_{DC}$  the reference dc-bias.

However, references for both Boosts *do not have to be independent*. The main disadvantage of the independent references is that the inverter output voltage ( $v_O$ ) is not directly controlled. As a consequence, this voltage can be affected by transient errors and dc offsets, and can show a poor rejection to external disturbances such as sudden load changes. A possible solution for this problem is to set an independent reference for one Boost, for instance the first one, and use the other Boost, the second one, to control directly the inverter output voltage, as shown by the following equations:

$$v_{O1ref} = V_{DC} + \frac{1}{\sqrt{2}}V \sin(2\pi ft) \quad (11)$$

$$v_{O2ref} = v_{O1} - v_{Oref} = v_{O1} - \sqrt{2}V \sin(2\pi ft). \quad (12)$$

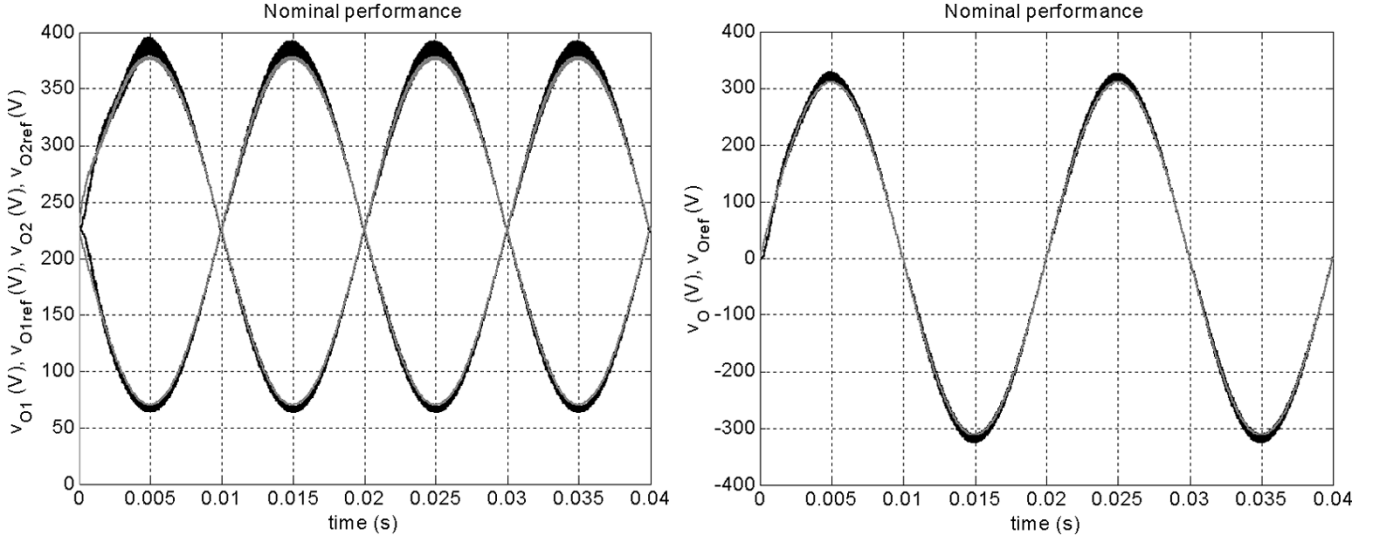


Fig. 4. Nominal simulation results.

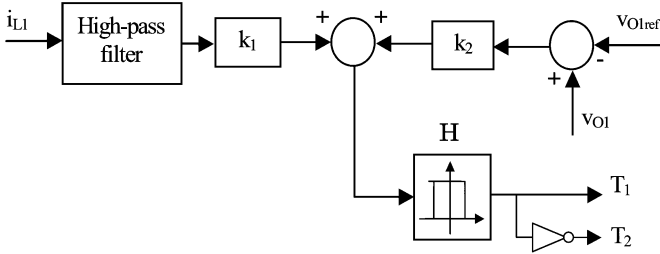


Fig. 5. Sliding mode control scheme.

With references given by (11) and (12), the second Boost controller can cancel inverter output voltage dc offsets and reject output voltage disturbances up to its control loop bandwidth.

Another option can be proposed that improves the system response in case of disturbances. Boost dynamics depends on the actual value of its duty cycle, which is obviously changing in this application. Fastest dynamics appear at the lowest levels of the duty cycles. Therefore, the Boost that has to compensate the output voltage variations can be selected depending on the sign of the sinusoidal output voltage. Then, the references for each Boost are now

$$if \sin(\omega t) > 0 \Rightarrow \begin{cases} v_{O1ref} = v_{O2} + v_{Oref} \\ \quad = v_{O2} + \sqrt{2}V \sin(2\pi ft) \\ v_{O2ref} = V_{DC} - \frac{1}{\sqrt{2}}V \sin(2\pi ft) \end{cases} \\ if \sin(\omega t) < 0 \Rightarrow \begin{cases} v_{O1ref} = V_{DC} + \frac{1}{\sqrt{2}}V \sin(2\pi ft) \\ v_{O2ref} = v_{O1} - v_{Oref} \\ \quad = v_{O1} - \sqrt{2}V \sin(2\pi ft) \end{cases} \quad (13)$$

The three options to generate Boost references explained above have been analyzed. The third option has been confirmed to achieve the quicker performance in load transients. However, an important restriction of this third option is its difficult physical implementation. Due to the necessary reference changes at the sinusoidal waveform zero crossings, small disturbances can then appear in the output voltage that can create small harmonics, especially in digital implementations with important

delays. In these systems, the second option should be chosen to be implemented.

#### IV. SIMULATION RESULTS AND COMPARISON WITH THE SLIDING MODE CONTROL

In order to validate the proposed control strategy, an IGBT-based Boost inverter prototype like the one shown in Fig. 1 has been designed, built and tested. The description of its physical implementation is given in Section V. The prototype inverter parameters and specifications are

$$\begin{aligned} L_1 = L_2 = 150 \mu\text{H} \quad C_1 = C_2 = 30 \mu\text{F} \\ P_N = 1.5 \text{ kW} \quad v_{IN} = 48 \text{ V} \\ V = 220 \text{ V} \quad f = 50 \text{ Hz} \\ V_{DC} = 226 \text{ V} \quad f_s = 20 \text{ kHz} \end{aligned} \quad (14)$$

where  $P_N$  is the inverter rated power,  $f_s$  the switching frequency and the rest of the elements were introduced in the previous sections. Equivalent series resistances of inductors and capacitors ( $r_{L1}$ ,  $r_{L2}$ ,  $r_{C1}$ , and  $r_{C2}$ ) are close to 10 m $\Omega$ .

The control strategy proposed in this paper is implemented on the prototype. Each Boost is controlled by means of the double-loop control scheme described before, and the voltage references for both Boosts are generated by means of the second option previously analyzed. An additional advantage of the proposed control strategy for the Boost inverter is that the dc voltage  $V_{DC}$  can be tuned as a function of the input voltage  $v_{IN}$ , as this voltage is measured by the control strategy. In this way, the output voltages of the Boosts achieve the minimum possible values, and then the switching losses are minimized for any input voltage  $v_{IN}$ .

The proportional-integral controller of the inner current control loop is designed in order to achieve a 50°-phase margin and a 4-kHz bandwidth. The proportional-integral controller of the outer voltage loop is calculated with the same phase margin and a 400-Hz bandwidth. These values make possible 50-Hz voltage references be accurately tracked.

Nominal operation simulation results of the Boost inverter when it is controlled by means of the control strategy proposed

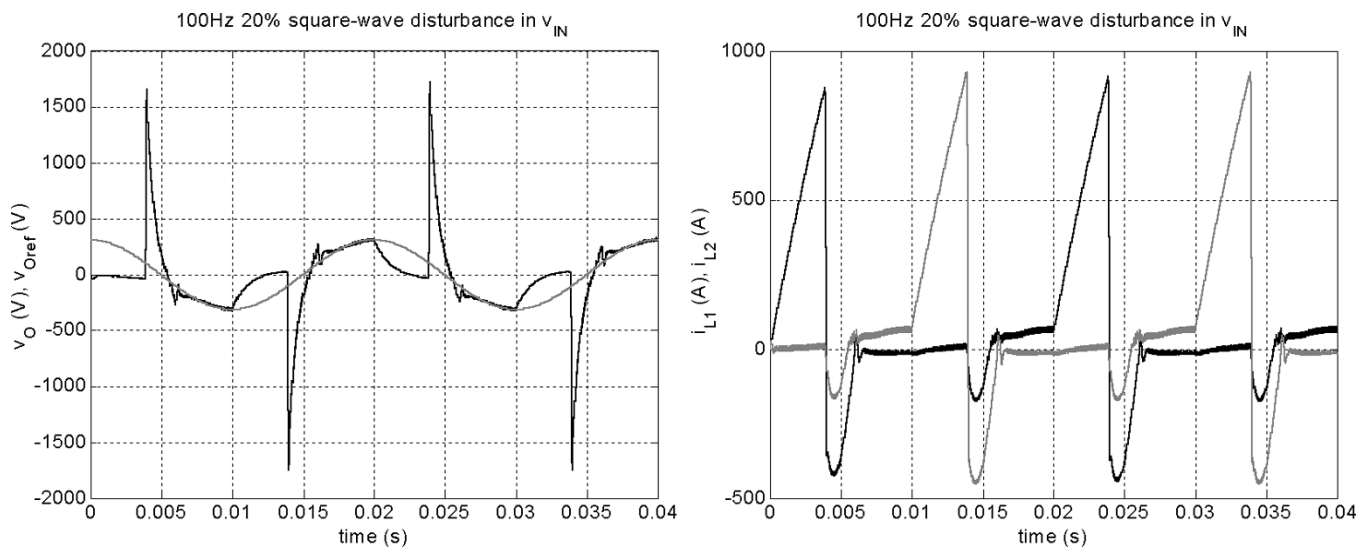


Fig. 6. Sliding mode control: robustness to a 100-Hz 20% square-wave disturbance in the input voltage.

in this paper are presented in Fig. 4. In this situation, the Boost inverter supplies a  $32.3\text{-}\Omega$  resistive load. These results show that the double-loop control scheme for each Boost obtains an accurate output voltage tracking with both Boosts working in a variable operation condition (graph on the left). As a consequence, the inverter output voltage is also accurately tracked (graph on the right).

As mentioned in the introduction, the sliding mode control has been proposed in the literature to control the Boost inverter. In order to compare this control with the control strategy proposed in this paper, a sliding mode controller is designed and implemented in both Boosts of the inverter. Basic scheme of the sliding mode control applied to Boost 1 is shown in Fig. 5. The sliding mode control defines a sliding surface that is a linear combination of inductor current and capacitor voltage errors, with coefficients  $k_1$  and  $k_2$ , respectively. This surface generates the switching pulses to the semiconductor devices by means of a hysteresis comparator. In principle, the switching frequency that results from this scheme is not constant. This can be a problem, although there are more complex implementations in which a constant frequency can be achieved. As it is not possible to know the current reference, the current error is calculated in the sliding mode control scheme as the high-frequency component of the inductor current. The main disadvantage of this current error calculation is the lack of control of the current average value, which can lead the current to reach high and dangerous values in some situations such as nonlinear loads, short circuit transients and strong load changes. The calculation of the control parameters  $k_1$  and  $k_2$  is restricted by the sliding mode existence and the system response fastness [2], [4]. For the Boost inverter prototype, the designed values of  $k_1$  and  $k_2$  are 0.0429 and 0.03, respectively.

The sliding mode control nominal simulation results are similar to those achieved by the proposed strategy. However, the robustness of the proposed control strategy to external disturbances is higher than that of the sliding mode control. Figs. 6 and 7 show the simulation results for both control strategies when a 100-Hz 20% square-wave disturbance is added to the input dc voltage. As it is observed, the sliding mode scheme becomes

unstable (Fig. 6) while the proposed strategy achieves a stable control of the inverter output voltage with a very fast response (Fig. 7). The sliding mode control does not control directly the inductor current, which reaches unavoidable values that would obviously activate the protections in a real system. As a consequence, the sliding controller fails to control the system. On the contrary, the inner current loop of the proposed strategy keeps the current under control limiting its value to the upper saturation limit of 100 A.

The reliability when supplying energy to a local electric network is one of the most important properties of a generation unit. The ability of the generation unit to overcome transient situations with no activation of its protections means a high quality, as it happens for instance in autonomous photovoltaic systems. Transient short circuits imply difficult situations for the inverters. The higher robustness of an inverter to these short circuits and its reliability in these situations will involve an important advantage in comparison with other inverters. There are many situations in which short circuits can appear. For instance, loads connected to the generation unit can fail causing thus a short circuit, the duration of which depends on the protection fuse time response. The sudden connection to the generation unit of electronic loads that include a diode bridge input stage with a discharged capacitor is another example of a transient short circuit situation. Even the starting of electrical motors and transformers can cause momentary short circuits.

In order to compare the reliability of the sliding mode control and the proposed control strategy, both control schemes have been tested in a transient short circuit operation. As it was mentioned before, an important disadvantage of the sliding mode control is the lack of control of the inductor current average value. As a consequence, the sliding mode control cannot cope with short circuit transients, and shows a very poor performance with nonlinear loads and abrupt load changes. In contrast with the sliding mode control, the new control strategy proposed in this paper does not have this problem due to the existence of an inner current control loop that controls the actual value of the inductor current and limits the maximum value of the inductor current.

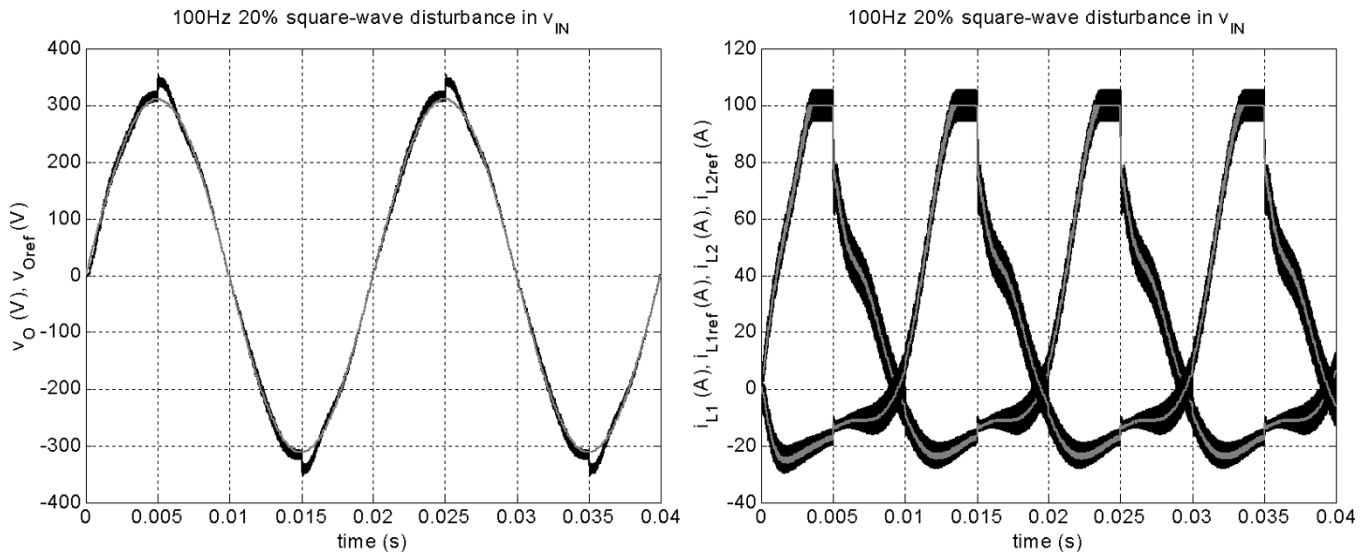


Fig. 7. Proposed control strategy: robustness to a 100-Hz 20% square-wave disturbance in the input voltage.

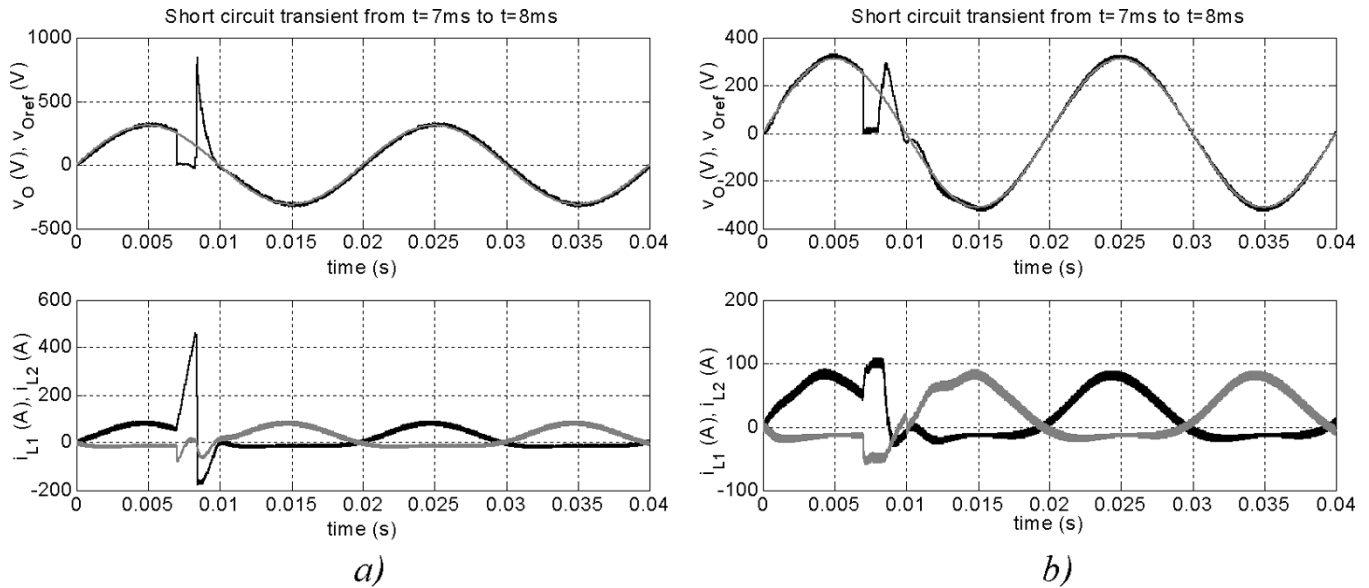


Fig. 8. Robustness to a transient short circuit: (a) sliding mode controller and (b) proposed control strategy.

Fig. 8 shows the robustness of both control strategies to a one second transient short circuit that occurs during the inverter nominal operation. Results show that the sliding mode controller is not able to overcome this situation. As it is shown in Fig. 8(a), the inductor current and output voltage reach very high values, up to 500 A and 800 V, that would activate the inverter overcurrent and overvoltage protections in a real system. On the contrary, the proposed control strategy keeps the system in a stable condition during the transient short circuit and recovers quickly the output voltage control when it finishes, as shown in Fig. 8(b). The inner current control loop makes possible the short circuit operation, with currents limited to their upper and lower saturation limits, 100 A and  $-50$  A, respectively. The absence of overcurrents and overvoltages avoid inverter protections be activated, and the system can go on operating after the short circuit situation, what means a very high reliability. In short, the proposed control strategy achieves a re-

liable, stable and fast control of the inverter output voltage even in these difficult operation situations.

## V. PROTOTYPE EXPERIMENTAL RESULTS

As it was indicated in the previous section, a Boost dc-dc inverter prototype has been physically implemented in order to test the satisfactory performance of the proposed control strategy. Two  $150\text{-}\mu\text{H}$  50-A rated rms-current inductors are used as inductors  $L_1$  and  $L_2$ , and two  $30\text{-}\mu\text{F}$  800-V rated dc-voltage electrolytic capacitors are used as capacitors  $C_1$  and  $C_2$ . The values for the rated power  $P_N$ , the input voltage  $v_{IN}$ , the reference dc-bias voltage  $V_{DC}$ , the output rms-voltage  $V$  and the output frequency  $f$  are the same as those specified in (14). Two Semikron SKM100GB123D modules each one of them consisting of two IGBTs and two diodes are used to build each Boost dc-dc converter [15]. Switching frequency  $f_s$

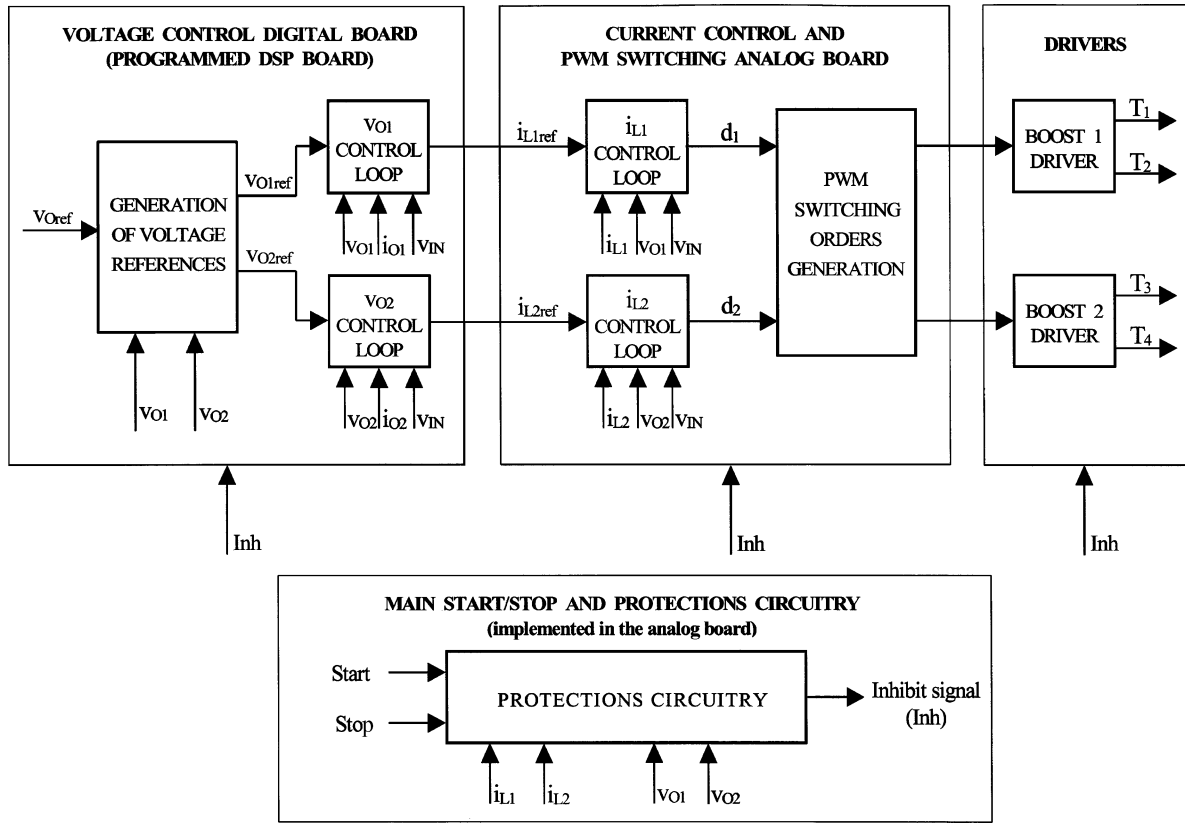


Fig. 9. Physical implementation block diagram of the control strategy on the Boost dc–ac inverter.

is 20 kHz, as given in (19). SKHI 23/12 double drivers from Semikron are used for the SKM100GB123D modules. On- and off-gate resistances ( $R_{Gon}$  and  $R_{Goff}$ ) are 15  $\Omega$ . The modules are mounted on a P16 heatsink also from Semikron.

Each Boost is controlled by means of the double-loop control scheme proposed in this paper. Fig. 9 shows the physical implementation block diagram of the control strategy. It consists mainly of a digital board that implements the voltage control loops, an analog board that implements the current control loops, and the IGBT drivers. The control parameters are the same as those indicated in the simulations. The bandwidth is 4 kHz for the current control loop and 400 Hz for the voltage control loop. 50°-phase margins are specified for both loops. With these parameters the proportional and integral constants of the current loop PI controller are 3.529 and  $8.44 \times 10^{-5}$ , respectively, while they are 0.059 and  $4.99 \times 10^{-4}$ , respectively, for the voltage loop PI controller.

The digital board is a dSPACE DS1102 board that operates in this case at a sample time of around 100  $\mu s$  [16]. This board is programmed to digitally implement the output voltage control loop proposed in Fig. 3 for both Boost dc–dc converters. It also generates the references  $v_{O1ref}$  and  $v_{O2ref}$  for the voltage control loops. These references are generated in order to control the inverter output voltage by means of the second option described by (11) and (12), that is, by driving a Boost with an independent reference and using the other Boost to directly control the inverter output voltage.

The analog board includes the current control inner loop proposed in Fig. 2 for both Boost dc–dc converters, as well as the PWM-switching orders generation. The current references

$i_{L1ref}$  and  $i_{L2ref}$  are obtained from the DSP board, where the voltage control loops are implemented. From the two inner current control loops, the duty cycles  $d_1$  and  $d_2$  are obtained, and the PWM switching orders are generated for the IGBT’s of both Boost dc-dc converters. Duty cycles are limited to 0.95 and 0.05.

Fig. 10 shows the electronic circuitry that implements the current control loop and the PWM-switching orders generation for the Boost 1. The circuitry for the Boost 2 is identical. The circuitry is divided into different blocks in order to make it clearer. A LEM LA125-P current sensor is used to measure the inductor current  $i_{L1}$  while two LEM LV25-P voltage sensors are used to measure the output voltage  $v_{O1}$  and the input voltage  $v_{IN}$ . Several TL084 are used as quadruple operational amplifiers and LM311 as voltage comparators. An AD632 from Analog Devices is used to implement the mathematical division required to compensate the output voltage  $v_{O1}$  and then obtain the duty cycle  $d_1$ . The PWM switching orders are generated by means of a Unitrode UC3637. Although in Fig. 10 only the A-outputs of this component appear as used, the B-outputs are also used in the analog board to generate the switching orders for the Boost 2. HEF4081B quadruple 2-input AND gates are used to cancel the switching orders in case of activation of the inhibit signal, which comes from the protections circuitry described below. Finally, the two SKHI 23/12 drivers receive the switching orders for the corresponding IGBTs  $T_1$  and  $T_2$ . These drivers have been included in Fig. 10 in order to make the circuit operation clearer.

Although the main start/stop and electronic protections circuitry has been represented as a different block in Fig. 9, these circuits are included in the analog board. Protections against overcurrents and overvoltages have been implemented as well

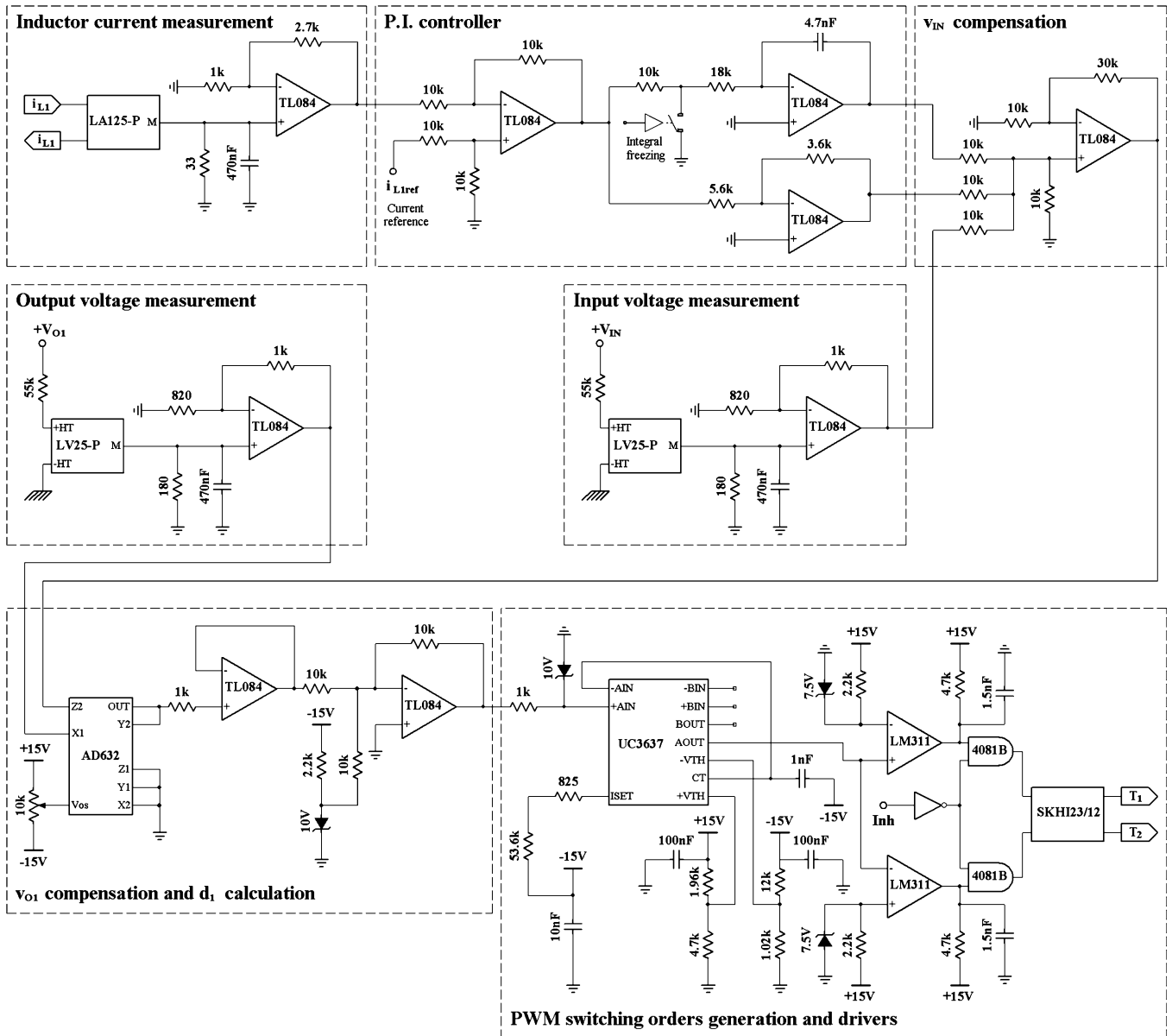


Fig. 10. Electronic circuitry that implements the current control inner loop of Boost 1 and the PWM switching orders generation for the corresponding IGBTs  $T_1$  and  $T_2$  (Circuitry for the Boost 2 is identical).

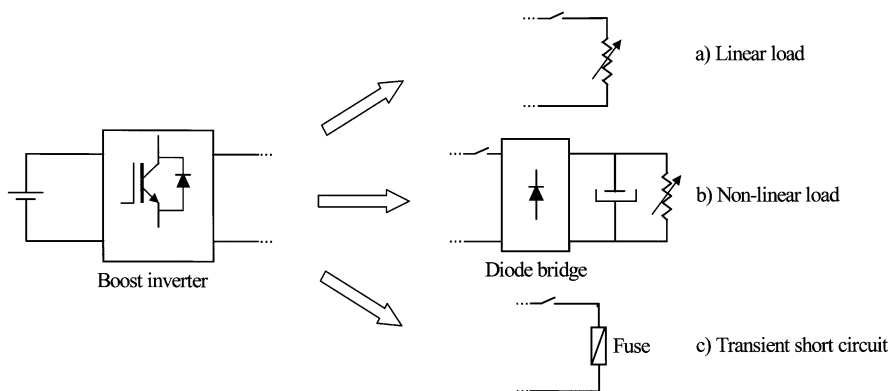


Fig. 11. Prototype experimental tests.

as against low signal dc supply voltage. If the protections or the main stop are activated, an inhibit signal ( $Inh$ ) is switched

on and the switching orders to the IGBTs are cancelled. The inhibit signal is also distributed to the control loops in order to



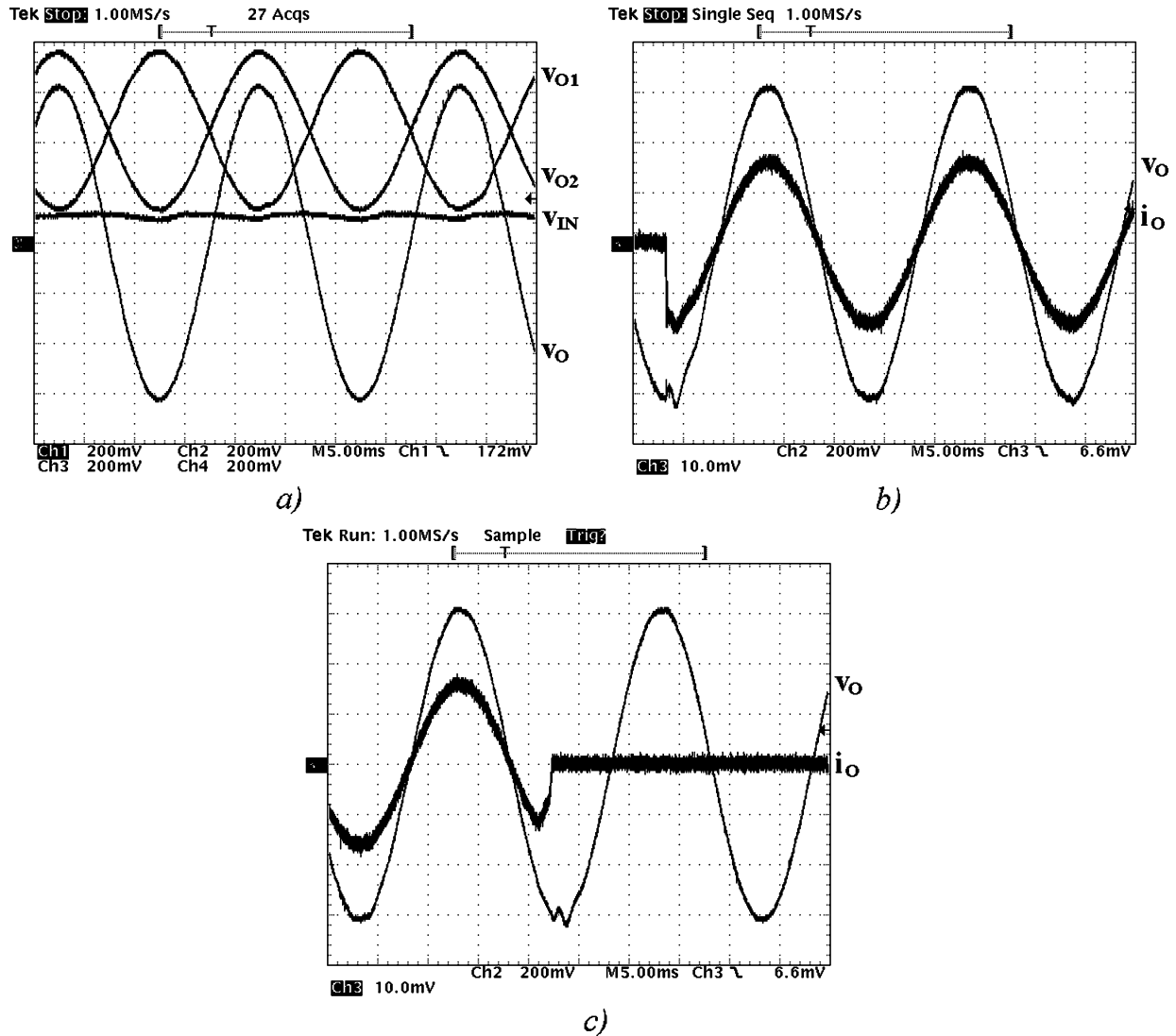


Fig. 12. Linear load experimental results (100- $\Omega$  resistive load): (a) nominal operation, (b) load connection, and (c) load disconnection ( $v_O$ ,  $v_{O1}$ ,  $v_{O2}$ ,  $v_{IN}$ : 100 V/div;  $i_O$ : 2 A/div).

make zero the controller outputs and references and be prepared for a later starting.

Fig. 11 shows the experimental tests carried out on the prototype. These tests include linear and nonlinear load operation (Fig. 11(a) and (b), respectively), and transient output short circuit performance [see Fig. 11(c)]. A Tektronix TDS 510 A oscilloscope is used to measure and capture the electrical variables.

Nominal operation results with a 100- $\Omega$  resistive linear load are shown in Fig. 12. Steady-state operation is presented in Fig. 12(a) while sudden load connection and disconnection are shown in Fig. 12(b) and (c), respectively. As expected from the simulations, both Boosts are successfully controlled in a variable operation condition, and the control strategy achieves a fast and accurate control of the inverter output voltage. The robustness to output current disturbance is shown in Fig. 12(b) and (c), where the load is suddenly connected and disconnected. The disturbance is satisfactorily rejected by the control strategy, even when it appears at the output voltage peak values.

The nonlinear load used in the nonlinear operation test consists of a diode bridge, a capacitor and a resistive dc load, as it was shown in Fig. 11(b). At present, this structure is quite

common as the input stage of electronic power supplies. Test results for the steady state operation are shown in Fig. 13(a), in which only the inductor current of Boost 2 is presented. The values for the capacitor and the load resistance are 235  $\mu\text{F}$  and 330  $\Omega$ , respectively, while the diode bridge is a Semikron SKB 30/08. In spite of the nonlinear load, the output voltage distortion that appears around the peak values is not important. These distortions are due to the capacitor charge, which means a quick transient short circuit. During these periods, inductor currents are effectively controlled inside their limits by means of the inner current loops, as can be observed in the second Boost inductor current waveform. The sudden connection of a nonlinear load represents a transient short circuit caused by the dc capacitor charge that finishes when this capacitor is charged. The bigger the capacitor is, the longer the short circuit lasts. Results of this connection are shown in Fig. 13(b), in which the value for the capacitor is now 470  $\mu\text{F}$  and the load resistance is not connected in order to show only the capacitor charge effect. As it is observed in the output voltage waveform, the connection of the nonlinear load and the capacitor charge process produces a short circuit operation that is controlled by means of the inner

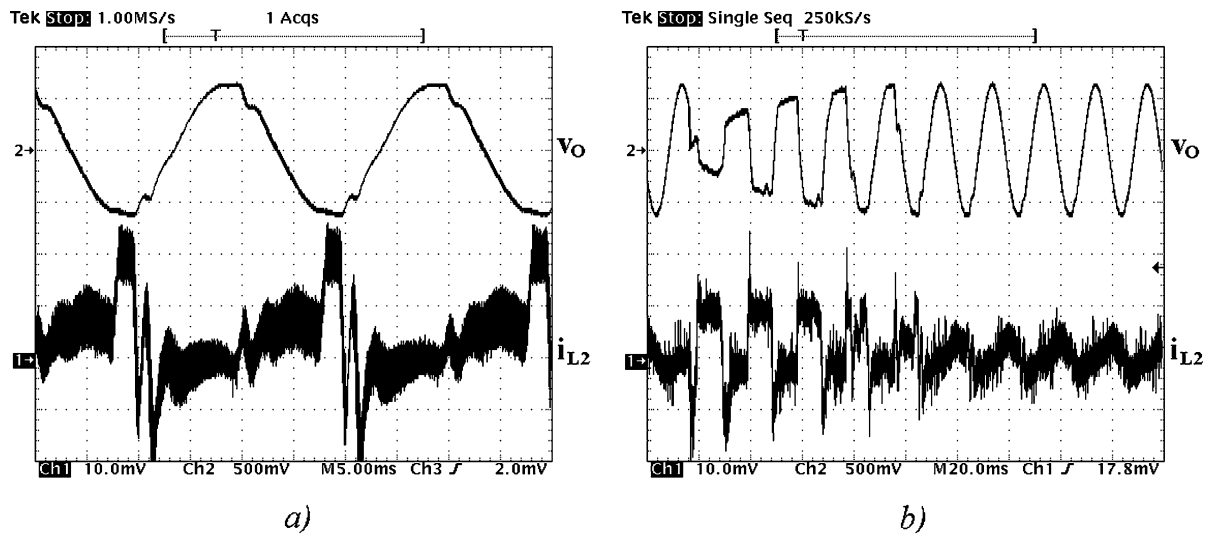


Fig. 13. Experimental results with a nonlinear load consisting of a diode bridge, a capacitor and a resistive dc load: (a) steady-state operation ( $v_O$ : 250 V/div;  $i_{L2}$ : 10 A/div) and (b) load connection ( $v_O$ : 250 V/div;  $i_{L2}$ : 20 A/div).

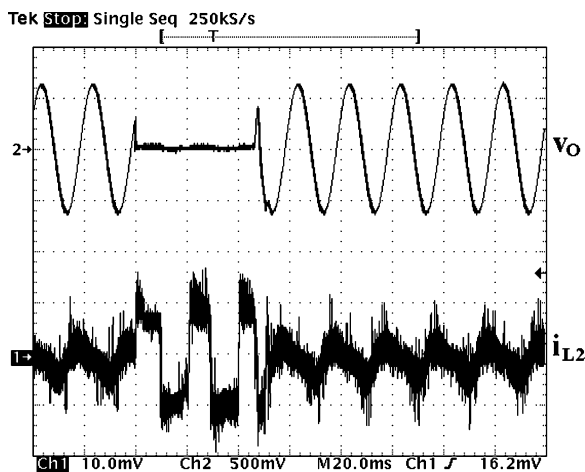


Fig. 14. Transient short circuit experimental results ( $v_O$ : 250 V/div;  $i_{L2}$ : 20 A/div).

current loops. The proposed control strategy achieves a stable control of the system and the current is limited avoiding thus the activation of the inverter protections. Once the capacitor is charged, the inverter output voltage control resumes to its steady state operation.

Finally, the system performance during an output short circuit is tested. This is the strongest test that can be applied to an inverter and shows the ability of the control strategy to overcome this situation without damaging the inverter or activating the overvoltage and overcurrents protections. The test has been carried out by suddenly short circuiting the output of the inverter through a fuse, as exposed in Fig. 11(c). The short circuit duration depends on the fuse melting time and the electric arc extinction. Results are shown in Fig. 14. As it is observed, the proposed control scheme achieves a stable inverter control even in this extreme situation. The inductor currents are permanently controlled to their limited values during the short circuit situation with no protections activation. Once the short circuit has finished, the system resumes almost immediately to the steady-state operation with no oscillations at all. In short, the proposed control strategy avoids protections shot during these

situations and then achieves a very high reliability. Anyway, depending on the desired inverter performance the protections shot can be programmed to be activated for long short circuits.

## VI. CONCLUSION

A control strategy for the Boost inverter has been proposed in this paper in which both Boosts of the Boost inverter are controlled by means of a double-loop control scheme that consists of a new inductor current control inner loop and an also new output voltage control outer loop. In order to deal with variable operation point condition of both Boosts, these loops include several compensations that make possible an accurate control of the Boosts. In addition, some feed-forward regulations are also designed that make the system highly robust to both input voltage and output current disturbances.

The proposed control strategy is validated both by simulation and prototype experimental results. In addition, it is compared with the sliding mode control. Nominal linear load performance is similar for both control strategies. However, the sliding mode control is not able to keep the system controlled under special transient situations, such as nonlinear loads, input voltage disturbances, and transient short circuits, while the proposed control strategy overcomes these situations with a robust, reliable and stable control of the system. In these situations, the sliding mode control becomes unstable and currents and voltages reach impossible values that would activate the protections in a real system. That means a very low reliability of the sliding-mode controlled system due, mainly, to the lack of control of the inductor current. On the contrary, the direct current control of the proposed control strategy makes possible to cope with these situations keeping the system under a stable operation condition with no overcurrents and overvoltages.

Tests carried out on the physical prototype controlled by means of the new control strategy proposed in this paper confirm the results obtained by simulation. Experimental tests include constant operation, connection and disconnection of both linear and nonlinear loads, as well as transient short circuits. The proposed control strategy achieves a stable, accurate and robust control in all these situations. Particularly, the

experimental prototype was tested in a short circuit situation in which the output was short-circuited during almost three cycles. As was exposed in the paper regarding the experimental waveforms, the proposed control strategy achieves a stable control of the system during the short circuit by means of limiting the inductor current to its programmed saturation value. After the short circuit, the system resumes to its nominal situation without any overvoltage or overcurrent. In short, the proposed control strategy achieves a very high reliability, what means a very valuable property of the generation unit. The so-controlled Boost inverter can be advantageously used in UPS, photovoltaic systems, etc.

## REFERENCES

- [1] R. Cáceres and I. Barbi, "A Boost DC-AC converter: operation, analysis, control and experimentation," in *Proc. IEEE IECON'95 Conf.*, Orlando, FL, Nov. 5–11, 1995, pp. 546–551.
- [2] R. O. Cáceres and I. Barbi, "A Boost dc-ac converter: analysis, design and experimentation," *IEEE Trans. Power Electron.*, vol. 14, no. 1, pp. 134–141, Jan. 1999.
- [3] M. K. Kazimierczuk, "Synthesis of phase-modulated dc/ac inverters and dc/dc converters," *Proc. Inst. Elect. Eng. B*, vol. 139, pp. 387–394, Jul. 1992.
- [4] R. O. Cáceres and I. Barbi, "Sliding mode controller for the Boost inverter," in *Proc. IEEE CIEP'96*, Cuernavaca, Mexico, Oct. 14–17, 1996, pp. 247–252.
- [5] N. Vázquez, J. Álvarez, C. Aguilar, and J. Arau, "Some critical aspects in sliding mode control design for the Boost inverter," in *Proc. IEEE CIEP'98 Conf.*, Morelia, Mexico, Oct. 12–15, 1998, pp. 76–81.
- [6] L. Dixon, "Average current mode control of switching power supplies," in *Proc. Unitrode Power Supply Design Sem. (SEM700)*, 1990.
- [7] R. D. Middlebrook, "Topics in multiple-loop regulators and current-mode programming," in *Proc. IEEE PESC'85 Conf.*, Toulouse, France, Jun. 24–28, 1985, pp. 716–732.
- [8] R. Naim, G. Weiss, and S. Ben-Yaakov, " $H_\infty$  control applied to Boost power converters," *IEEE Trans. Power Electron.*, vol. 12, no. 4, pp. 677–683, Jul. 1997.
- [9] P. Sanchis Gúrpide, O. Alonso Sádaba, and L. Marroyo Palomo, "Variable operating point robust control strategy for Boost converters," in *Proc. 9th Eur. Conf. Power Electronics Applications (EPE'01)*, Graz, Austria, Aug. 27–29, 2001.
- [10] P. Sanchis Gúrpide, O. Alonso Sádaba, L. Marroyo Palomo, T. Meynard, and E. Lefeuvre, "A new control strategy for the Boost dc-ac inverter," in *Proc. IEEE PESC'01 Conf.*, Vancouver, Canada, Jun. 17–21, 2001, pp. 974–979.
- [11] R. D. Middlebrook and S. Cuk, "A general unified approach to modeling switching-converter power stages," in *Proc. IEEE PESC'76 Conf.*, Cleveland, OH, Jun. 8–10, 1976, pp. 18–34.
- [12] M. K. Kazimierczuk and A. Massarini, "Feedforward control of dc-dc PWM Boost converter," *IEEE Trans. Circuits Syst. I Fundam. Theory Appl.*, vol. 44, no. 2, pp. 143–148, Feb. 1997.
- [13] M. K. Kazimierczuk and L. A. Starman, "Dynamic performance of PWM dc-dc Boost converter with input voltage feedforward control," *IEEE Trans. Circuits Syst. I*, vol. 46, no. 12, pp. 1473–1481, Dec. 1999.
- [14] J. A. Weimer, M. K. Kazimierczuk, A. Massarini, and R. C. Cravens, "Feedforward control of aircraft bus ac Boost converter," U.S. Patent 5982 156, Nov. 9, 1999.
- [15] Semikron. (2003) Semikron Databook 2003, Nuremberg, Germany. [Online] Available: <http://www.semikron.com>
- [16] dSPACE. (2004) dSPACE Catalogue 2004. [Online] Available: <http://www.dspace.com>



**Pablo Sanchis** (M'03) received the M.Sc. degree in management and business administration, and the M.Sc. and Ph.D. degrees in electrical engineering from the Public University of Navarra, Pamplona, Spain, in 1994, 1995, and 2002, respectively.

From 1996 to 1998, he was a Guest Researcher at Delft University of Technology, Delft, The Netherlands, on the field of control of electrical machines. Since 1998, he has been an Assistant Professor at the Department of Electrical and Electronic Engineering, Public University of Navarra, where he has also been involved in many research projects mainly in co-operation with industry. His research interests include power electronics, distributed generation, control of power converters, photovoltaic and hybrid systems, alternative energy systems, and hydrogen generation from renewable sources.



**Alfredo Ursæa** (M'04) received the B.S. (with honors) and M.S. (with honors) degrees in electrical engineering from the Public University of Navarra, Pamplona, Spain, in 2001 and 2004, respectively, where he is currently pursuing the Ph.D. degree.

In 2002, he was a Researcher with the Department of Electrical and Electronic Engineering, Public University of Navarra, Spain. In 2003, he joined this department as an Assistant Professor. Since 2002, he has been involved in several research projects mainly related to alternative energy systems. His

interests concern hydrogen generation from renewable energy sources, power electronics, and photovoltaic systems.



**Eugenio Gubía** (M'04) received the M.Sc. and the Ph.D. degrees in industrial engineering from the Public University of Navarra, Pamplona, Spain, in 1995, and 2003, respectively.

In 1996, he joined the Power Electronic Group, Electrical and Electronic Department, Public University of Navarra, where he is currently an Assistant Professor and is also involved in research projects mainly in co-operation with industry. His research interests are in the field of renewable energies, power converters, electrical power systems

quality, and EMI.



**Luis Marroyo** (M'04) received the M.Sc. degree in electrical engineering from the University of Toulouse, France, in 1993, the M.Sc. degree in electrical engineering from the Public University of Navarra, Pamplona, Spain, in 1997, and the Ph.D. degree from the LEEI-ENSEEIH T INP Toulouse, France, in 1999.

From 1993 to 1998, he was Assistant Professor with the Department of Electrical and Electronic Engineering, Public University of Navarra, where he has been an Associate Professor since 1998. His

research interests are in power electronics, grid quality, and renewable energy.